Eleventh International Conference on CFD in the Minerals and Process Industries
CSIRO, Melbourne, Australia
7-9 December 2015

NUMERICAL VALIDATION OF THE EISFELD AND SCHNITZLEIN PRESSURE DROP CORRELATION FOR SMALL ASPECT RATIO PACKED BEDS

J.H. KRUGER*, C.G. DU TOIT and W.J.S. VAN DER MERWE

[1] School of Mechanical and Nuclear Engineering, North-West University, Potchefstroom, SOUTH AFRICA
*Corresponding author, E-mail address: janhendrik.kruger@nwu.ac.za

ABSTRACT

Packed beds consisting of spherical particles are widely used in the minerals and process industries, with typical applications ranging from chemical reactors to nuclear heat generation. The pressure drop of a fluid flowing through the packed bed is of critical importance for the successful design and operation of installations.

Four factors mainly influence the pressure drop: the fluid and flow properties typically characterized by the Reynolds number, the porous structure and the bed geometry, typically characterized amongst others by the aspect ratio. With small aspect ratio (ratio between cylinder diameter and particle diameter) beds, it was further found that the vessel walls affect the porous structure close to the boundaries. This leads to significant "wall effects" involving the local flow resistance and heat transfer processes between the bed and vessel walls.

The Eisfeld and Schnitzlein (ES) correlation is a popular Ergun-type correlation used to predict the pressure drop over packed beds with small aspect ratios. The parameters of the ES correlation were derived from an in-depth analysis of results from a large number of experiments conducted using suitable bed geometries.

To validate the ES correlation numerically, a CFD based methodology was developed in this study. Packed beds with different aspect ratios were packed with spheres using the Discrete Element Method (DEM) and the interstitial spaces between spheres were discretized to obtain the numerical flow domain. From the CFD simulations, the pressure drops and friction factors over the beds were obtained, which were subsequently compared with the values predicted by the ES correlation.

Excellent agreement was found between the ES correlation and numerical results for the range of Reynolds numbers and aspect ratios investigated. This increased confidence in the numerical methodology as well as in the use of the ES correlation to predict the pressure drop of turbulent flow over packed beds with small aspect ratios.

NOMENCLATURE

a, a', b, b'	Proportionality constants
B	Mesh base size
D	Cylinder diameter
D_C	Diameter of contact area
d	Particle diameter
E, E'	Wall effect functions
f	Fillet radius
k	Turbulent kinetic energy
L	Length of final bed
L_{DEM}	Length of DEM bed
L_I	Inlet length of bed
L_O	Outlet length of bed
N	Number of particles
n	Ergun equation constant
p, p_a	Pressure, Ambient pressure
Δp	Pressure drop
$\mathrm{Re_m}$, $\mathrm{Re_p}$	Reynolds number (modified, particle)
T_a	Ambient temperature
U	Bulk velocity
y	Coordinate in the y-direction
α	Aspect ratio
ε	Dissipation rate of turbulent kinetic energy
ε_b	Bulk bed porosity
γ	Turbulence velocity intensity
μ	Dynamic viscosity
μ^τ	Turbulent viscosity
ρ	Density
Ψ	Friction factor

INTRODUCTION

A packed bed can be described as any fixed container that is packed with particles, where the particles can vary in shape and size. The basic principle of all packed beds is that a working fluid is passed through the particle bed, between the particles, causing numerous flow, thermal and chemical effects. Many processes in the minerals and process industries take advantage of the favourable flow conditions in a packed bed, e.g.: filtration, ion exchange, drying, heterogeneous catalysis, thermal heat exchangers and nuclear packed bed reactors (Dolejs and Machac, 1995; Mueller, 2010).

When considering the design of any thermo-hydraulic system that incorporates a packed bed, the pressure drop over the bed is one of the most important variables that must be predicted accurately (Winterberg and Tsotsas, 2000), as it is related to the flow distribution, pumping power and operating costs (Hassan and Kang, 2012). For these basic design reasons, the flow through packed beds has been the topic of interest for many authors. Ergun (1952) was one of the first authors to summarise the factors which influence the pressure drop over packed beds as: (1) the rate of fluid flow, (2) viscosity and density of the fluid, (3) closeness and orientation of the packing, and (4) size, shape and surface roughness of the particles. Hence, the pressure drop is very sensitive to the geometrical properties of the bed.

The focus in this study was on cylindrical beds with small aspect ratios containing mono-sized, loosely packed spherical particles. The most important geometric properties considered were:

(i) The aspect ratio α:

$$\alpha = D / d \tag{1}$$

with D the cylinder diameter and d the particle diameter and with a value of $\alpha \leq 10$.

and (ii) the bulk bed porosity ε_b:

$$\varepsilon_b = \frac{\text{Volume of the voids}}{\text{Total volume}} = 1 - \frac{\text{Volume of the solids}}{\text{Total volume}} \tag{2}$$

which gives an indication of the permeability of the bed.

In randomly packed beds with large aspect ratios, the porosity can be considered uniform and designers assume that the flow distribution is uniform over the cross-section of the bed (Eppinger et al., 2011). However, particles form ordered packing structures on the bed boundaries, which result in large variations in porosity in the near-boundary regions. This phenomenon is commonly known as the wall effect, and becomes increasingly prominent at smaller aspect ratios (De Klerk, 2003; Mueller, 2010).

For the purpose of this study, the limiting value of 10 was chosen to define the term "small" aspect ratio, as previous researchers found that the wall effect dampened out after roughly 5 particle diameters from the wall, signifying the transition from "small" to "large" aspect ratio at a cylinder diameter of 10*d* (Benenati, 1962; Mariani, 2009).

Since the wall effect is related to the bed permeability, the flow distribution therefore should not just be assumed to be uniform over the diameter of finite beds. However, the wall effect presents numerous difficulties when attempting to predict the pressure drop, as it is Reynolds number dependent (Cheng, 2011). In creeping flow regimes, a decrease in the aspect ratio leads to an increase in the pressure drop, due to additional friction. In turbulent flow regimes however, a decrease in the aspect ratio leads to a decrease in pressure drop, due to higher porosity (Di Felice and Gibilaro, 2004; Reddy and Joshi, 2008).

The most common method to predict pressure drop uses a hydraulic diameter approach to calculate the bed friction factor, which is analogous to the flow through pipes. Researchers who first used this method to predict the pressure drop over infinite beds, were Carman (1937) and Ergun (1952). Their correlations, however, do not take the wall effect into account and present inaccurate predictions at low aspect ratios.

Types of pressure drop equations

Reynolds (1900) was the first to correlate the resistance offered by friction to the motion of the fluid as the sum of the viscous and kinetic energy losses:

$$\frac{\Delta p}{L} = a\mu U + b\rho U^n \tag{3}$$

where $a\mu U$ represents viscous energy losses, $b\rho U^n$ kinetic energy losses, and $n = 2$.

Ergun (1952) expressed the viscous and kinetic energy proportionalities as:

$$a = a' \cdot \frac{(1-\varepsilon_b)^2}{\varepsilon_b^3} \quad ; \quad b = b' \cdot \frac{(1-\varepsilon_b)}{\varepsilon_b^3} \tag{4}$$

where values for a' and b' were obtained empirically.

Substituting eq. (4) into eq. (3), and rewriting in terms of the friction factor for the general case yields:

$$\Psi = \frac{\Delta p}{\rho U^2} \cdot \frac{d}{L} \cdot \frac{\varepsilon_b^3}{1-\varepsilon_b} = \frac{a'}{\text{Re}_m} + \frac{b'}{(\text{Re}_m)^{2-n}} \tag{5}$$

Eq. (5) is the most general form of the friction factor for fluid flow through packed beds with two main variations:

(i) Ergun-type equations: Ergun-type equations are variations of eq. (5) for which $n = 2$, as originally proposed by Reynolds (1900). These equations are arguably the most widely used for pressure drop.

(ii) Carman-type equations: Carman-type equations are variations of eq. (5) for which $1.9 \leq n \leq 1.95$, as proposed by Carman (1937).

The KTA correlation and its limiting line

During German development of the Gas-Cooled Pebble-Bed Modular Reactors, the Nuclear Safety Standards Commission, “Kerntechnischer Ausschuss” (KTA), made considerable effort to develop a Carman-type equation to predict the pressure drop over packed beds with mono-sized spherical particles (KTA, 1988). The derivation of this correlation took experimental investigations from various authors and chose data points where the influence of the containing walls was negligible. By plotting the values for aspect ratio against Reynolds number, they estimated a limiting line for the region where wall effects were negligible.

The KTA correlation is widely used in industrial packed bed design and analysis, but by definition is not valid for small aspect ratios and the theoretical basis for its limiting line is unclear. The need was thus identified to further investigate and numerically validate equations such as the ES-correlation to improve the body of knowledge for the regions not properly covered by the KTA correlation.

The Eisfeld and Schnitzlein correlation

The Eisfeld and Schnitzlein (ES) correlation is an Ergun-type equation derived from more than 2300 experimental data points (Eisfeld and Schnitzlein, 2001). This correlation was specifically investigated in this study as it takes the wall effect into account and predicts accurate values for the friction factor at low aspect ratios.

Assuming an Ergun-type equation to be valid, they determined values for the constants in the Reichelt (1972) version of the Ergun correlation, to obtain the best fit for the correlation’s predictions to the experimental data. It was found that their improved correlation does not degrade for small aspect ratios of $\alpha \leq 10$. Eqns. (6) and (7) show the correlation proposed by Reichelt (1972), with the modifications by Eisfeld and Schnitzlein (2001), where E and E' are functions that account for the wall effect.

Eisfeld and Schnitzlein (2001) found the constants to be $e = 154$, $e' = 1.15$ and $e'' = 0.87$ for spherical particles.

$$\psi_{ES} = \frac{e \cdot E^2}{\mathrm{Re}_p} \cdot (1 - \varepsilon_b) + \frac{E}{E'} \quad (6)$$

$$E = 1 + \frac{2}{3\alpha(1-\varepsilon_b)} \quad ; \quad E' = \left(e'\alpha^{-2} + e''\right)^2 \quad (7)$$

Eqns. (6) & (7) were found to be valid within:

- Reynolds number: $0.01 < \mathrm{Re}_p < 17635$.
- Porosity: $0.33 < \varepsilon < 0.882$.
- Aspect ratio: $1.624 \le \alpha \le 250$.

In the current study, packed beds were generated using DEM, and the flow through the beds simulated using CFD. STAR-CCM+ was used for both DEM and CFD operations. The results from this explicit approach were firstly validated with empirical data from Wentz and Thodos (1963) and then finally compared with the Eisfeld & Schnitzlein correlation's predictions.

Discrete Element Method

First introduced by Cundall and Strack (1979), the Discrete Element Method (DEM) is an explicit numerical scheme that simulates the dynamic and static behaviour of assemblies of particles based on contact mechanics. It is usually assumed that particles displace independently, interact only at contact points and are rigid bodies. (DEM requires only discretized surfaces and not a fluid volume).

With regard to DEM used in studying packed beds, Eppinger et al. (2011) generated randomly packed beds by initialising spherical particles within a cylindrical domain, which dropped to the bottom of the tube due to gravity. Good agreement was found for global bed porosity and radial porosity distributions between their DEM results and results from literature.

Computational Fluid Dynamics combined with DEM

The complexities in the structure of packed beds have so far prevented the detailed understanding of the flow between bed particles. With recent increases in computational power, Computational Fluid Dynamics (CFD) has become a viable method to analyse the complex flow conditions in packed beds (Reddy and Joshi, 2010). Such CFD analyses require three-dimensional (3D) models of the particle geometry, and the Discrete Element Method (DEM) has shown promise to generate realistic randomly packed beds (Eppinger et al., 2011).

Theron (2011) investigated a methodology to model the flow through packed beds using an explicit approach. Using DEM, the author generated beds with aspect ratios of $1.39 \le \alpha \le 4.93$, and simulated the flow through each bed. His results for porosity and pressure drop compared well with that found in literature. Theron (2011) showed that the multi-physics simulation software package STAR-CCM+ (CD-Adapco, 2012) provides a stable platform for combined DEM and CFD operations, as is utilized during the analysis of packed beds.

Simulation setup methodology

Due to limitations in the interaction of the DEM and CFD modules of STAR-CCM+, a specific methodology was required in order to generate the final fluid volume of the packed beds used in CFD pressure drop calculations.

The DEM and CFD modules use separate surface meshes to define the outer boundaries of the domain (in this case the outer cylinder). Particle movement was calculated in the DEM module and when completed, only the centre coordinates of spheres were exported to a CAD package.
In the CAD modelling package the sphere surfaces were created and the contact treatment was performed. The resulting particle surface was combined with an outer cylinder surface and exported to the CFD module.

These steps were necessary since the version of STAR-CCM+ used for this investigation was not yet capable of directly converting DEM particles to solid bodies/boundaries. The software also did not provide the solid modelling tools needed to perform contact treatment.

DEM SIMULATION SETUP

Geometrical domain and boundaries

The basic cylindrical DEM domain had a diameter equal to the cylinder diameter of the final bed, D, and a total axial length of L_{DEM}. The cylinder- and particle surfaces were set as wall boundaries, with no slip. To accommodate particle generation, L_{DEM} was made 20% larger than the expected length of the final bed, L. Thus, $L_{DEM} = 1.2(L/d)$ where $L/d = 10$ in order to keep L_{DEM} as short as possible to speed up calculations.

Particle injection and the mesh continua

Particles were generated at the top of the domain using a point injector, and simulated to fall in the *z*-direction under a gravitational influence. The point injector was set on the cylinder centreline, one particle diameter from the top.

For DEM applications, a coarser mesh resolution (roughly a quarter particle diameter in this case) can be used when compared to typical CFD applications, since only discrete particles are tracked - not the fluid movement itself. The boundary surface of the mesh must however still be refined to prevent undesirable curvature deviation from the original cylinder boundary by the coarser mesh.

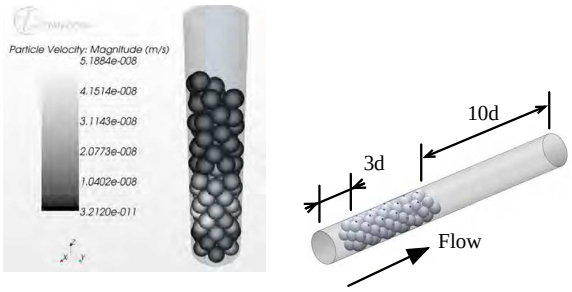

(a) DEM particles (b) CFD simulation domain

Figure 1: Examples of (a) finished DEM simulation and (b) domain created for CFD simulations.

Stopping criteria

DEM simulations are inherently transient and an implicit unsteady time step of 0.05s and a DEM time scale of 0.05s were set within the implicit unsteady simulation model. Particle-to-particle and particle-to-wall interaction models were activated and the built-in Hertz-Mindlin contact model was used (CD-Adapco, 2012).

Particles were generated at a rate of one particle per second and the maximum physical time was specified as the number of expected particles to be generated, plus three seconds. The extra three seconds was found by Van der Merwe (2014) to be sufficient to allow for settling of the bed under gravity. This means that the DEM generated beds had loose packing structures, since no vibration of the container was simulated after the particles settled. An example of packing for an aspect ratio of 3.0 is shown in Fig. 1(a), with typical settling velocity magnitudes.

CFD SIMULATION SETUP

Geometrical domain

Domains for the CFD simulations of the flow through the beds were created using the CAD software package SolidWorks, by importing the centre coordinates of the particles obtained from the DEM simulations. Fig. 1(b) shows an example of the domain as created in SolidWorks, for a bed with aspect ratio of $\alpha = 3.00$. These domains were created with the inlet region protruding a length of $L_I = 3d$ from the bed and the outlet region extending a length of $L_O = 10d$ from the bed. The contact treatment was also applied as will be discussed later. The solid domains created in SolidWorks were then imported into STAR-CCM+ as surface meshes.

Boundaries

The domains imported into STAR-CCM+ were split into four different regions, with boundary conditions illustrated in Fig. 2 for a typical bed with $\alpha = 6.33$. The inlet boundary was defined as a velocity inlet, the outlet boundary as pressure outlet, the cylinder's inner surface as a wall with no slip and the particles' surfaces also as wall boundaries with no slip.

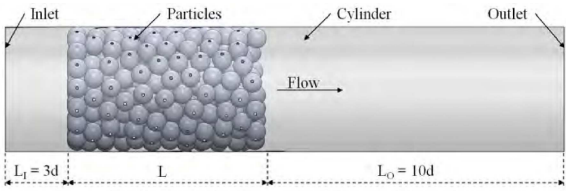

Figure 2: Illustration of the regions specified for the CFD simulations, for a bed with $\alpha = 6.33$.

A realistic representation of the flow entering a packed bed is fully developed viscous flow. Velocity profiles for fully developed laminar and turbulent flows were calculated using standard analytical solutions from Munson et al. (2010, p. 407). These velocity profiles were specified at the inlet boundaries as a function of the radial coordinate, *r*. In the case of turbulent flow, a viscosity ratio of $\mu^{\tau}/\mu = 10$ and turbulence velocity intensity of $\gamma = 0.01$ were also specified.

Also note that the assumption was made that the control volume was adiabatic, thus no heat transfer over the boundaries was allowed. The default reference values for ambient temperature of $T_a = 300$ K and ambient pressure of $p_a = 101.325$ kPa were used to determine fluid properties in all simulations.

Mesh & Physics Continua

The detailed mesh independency study by Van der Merwe (2014), determined the optimum meshing models and parameters for the problem dimensions and range of Reynolds numbers examined in this study. The models used were: surface remesher, polyhedral volume mesher and prism layer mesher. Table 1 gives the relative values of the significant parameters used for the mesh generation.

PARAMETER	VALUE
Base size, B	1.7 mm < *B* < 2.0 mm
Surface size, minimum	0.25*B*
Surface size, target	1.00*B*
Number of prism layers	2
Prism layer thickness	0.20*B*

Table 1: Mesh generation parameters.

It should be noted that the same prism layer settings were applied to the surface meshes on the particles as well as on the cylinder walls so that wall-effects in the boundary flow were captured adequately. In Fig. 3 the relation between particle count and total number of cells is shown and it can be seen that the cell count rapidly increases as the physical size (and thus aspect ratio) of the bed increases.

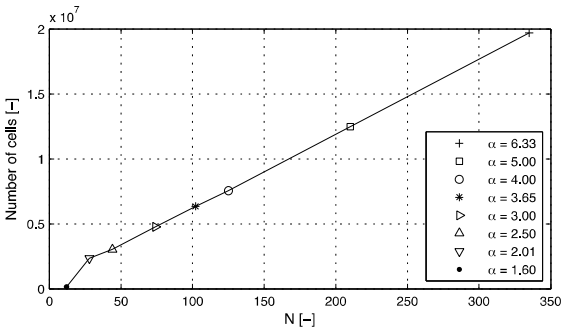

Figure 3: Number of cells generated for each bed as a function of the number of particles in the bed, *N*.

To identify a suitable turbulence solver, the decision was made to compare the pressure drop results from the least complex and most complex turbulence models with each other and with the correlations. The rationale being, that if the least computationally intensive model gives acceptable results, it would suffice for practical applications. Furthermore, in packed bed applications there is no need to model laminar-to-turbulent transition as the flow is already fully turbulent upon entry to the bed.

Thus a comparative study of pressure drop values across the reference bed was completed using the standard Realisable $k-\varepsilon$ model and the much more computationally intensive Large-Eddy-Simulation (LES) model. The differences in Δp between $k-\varepsilon$ and LES (30s at $\mathrm{Re}_p = 10^3$) was 0.77% for the first case and 1.01%

between $k-\varepsilon$ and LES (the second case: 3s at $\mathrm{Re}_p = 10^4$). These small differences did not justify the additional computational effort required by LES, thus it was decided to use the Realisable $k-\varepsilon$ model as the turbulence solver in the current investigation.

From this investigation of the influence of different turbulence models, and the best practices suggested by CD-Adapco (2012), the physics models used for all CFD simulations were chosen as: steady state flow, coupled implicit solver, air as ideal gas, turbulent flow with Realisable $k-\varepsilon$ model and two-layer all y+ wall treatment.

Contact treatment

A crucial point for the mesh generation in packed beds is the cell quality near the contact points between particles, and between particles and the cylinder wall. Due to its geometric nature, the contact points force the flow area around it to be very small, thin and acute. The cells near the contact points are usually either highly skewed or highly refined. High numbers of skewed cells lead to convergence problems during the calculation, whereas highly refined regions increase the number of cells and, as a direct consequence, the computational time (Eppinger et al., 2011). Thus, a balance between these two extremes must be found, especially when bed sizes are increased.

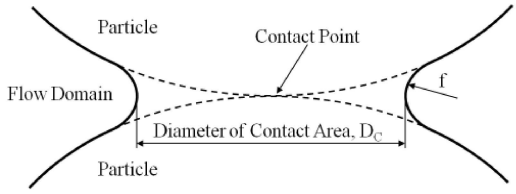

Figure 4: Schematic illustration of a contact point between two particles with a filler radius *f*.

Several methods to overcome this problem exist, of which the approach followed by Reyneke (2009) was found the most suitable one by Van der Merwe (2014). Particles were connected to each other without changing the particle diameter. This was achieved by creating a fillet, with a specified radius of curvature *f*, on all intersection points between particle-particle and particle-cylinder surfaces, as shown in Fig. 4. This approach results in a realistic flow situation and provides a method usable for future research into the detail heat transfer between particles.

Solvers and stopping criteria

Due to the complex nature of the flow of the compressible fluid between the particles, the coupled implicit solver's Courant number was given a value 1.0. In order to decrease convergence time, the Continuity Convergence Accelerator (CCA) was also enabled, with an under relaxation factor of 0.01. Simulations were accepted as converged when all residual values were smaller than 10^{-3}, and a steady state calculation was achieved.

REFERENCE PACKED BED SETUP

The reference packed bed was used to develop the methodology and all the beds for different aspect ratios were generated and analysed in a similar manner.

Geometry

The reference bed contained N = 10 particles and had an aspect ratio of α = 2.01. Fig. 5 shows a schematic of the bed, with flow direction, particle locations and inlet/outlet. The cylinder diameter was 100.00 mm, particle diameter was 49.80 mm, L_I was 50.00 mm and L_O was 250.00 mm.

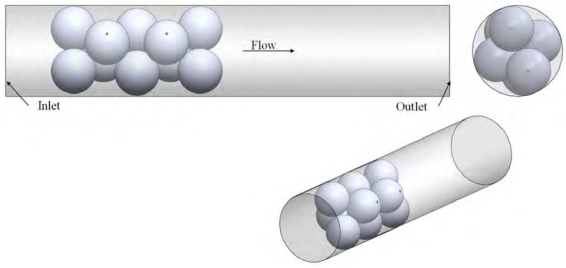

Figure 5: Reference bed used for the development of the methodology.

Mesh independence

The mesh independency study found a deviation of < 1.0% in Δp going from a 1.4 mm mesh base size to 2.0 mm base size. This indicated that 1.7 mm < B < 2.0 mm would be an appropriate mesh density to use. An investigation of the effect of fillet radius on pressure drop further found that for a radius f = 0.1 mm, Δp was a minimum. This value for f thus exhibited the smallest influence on fluid flow but still limited the number of low quality cells in the mesh.
In Fig. 6 the typical mesh structure in the reference bed is shown together with detail on the mesh surrounding the fillet area between two particles.

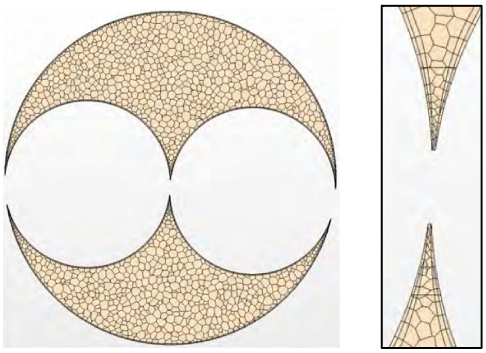

(a) Mesh base size B = 2 mm. (b) f = 0.1 mm.

Figure 6: (a) Mesh structure in the reference bed, with B = 2.0 mm. (b) Mesh structure at a contact point between two particles with f = 0.1 mm.

Pressure drop measurement

It was found that a region with negative pressure forms just after the particles, and extends for approximately five particle diameters towards the outlet, after which it recovers to atmospheric pressure. This low-pressure region formed due to vortices after the last particles.

Because of the localised recovery of static pressure, and the region with negative pressure just after the particles, it was decided to take the measurement of the pressure drop over the bed as the pressure difference between the pressure at the inlet boundary and atmospheric pressure. This method is similar to that employed by Eppinger et al.

(2011), Reddy and Joshi (2010) and Bai et al. (2009) and ensured that the calculations of Δp would not be influenced by local pressure variations.

RESULTS

The Wentz and Thodos correlation

Wentz and Thodos (1963) did thorough experiments on the flow through structured packed beds consisting of mono-sized spherical particles of 1.23in diameter. They took pressure drop measurements for the flow through beds arranged in cubic, body-centred cubic and face-centred cubic orientations. Their beds were made of plastic phenolic spheres, which were fixed in space with short lengths of wire. Each packing arrangement had five layers of particles in the axial direction. The beds were machined to fit into a cylindrical wind tunnel by removing excess portions of the external spheres, to eliminate the wall effect.

The pressure drop across a single layer of particles in the middle of each bed was taken, to eliminate any entrance and exit effects. From these measurements, the following correlation was obtained:

$$\Psi = \frac{0.351}{\mathrm{Re}_m^{0.05} - 1.2} \tag{8}$$

Fig. 7 shows the pressure drops predicted by the CFD simulations as well as the experimental measurements by Wentz and Thodos (1963). A deviation from the measured pressure drop by Wentz and Thodos (1963) can be observed at $\mathrm{Re_m} \approx 13200$ in Fig. 7(a). This deviation could be attributed to experimental error, however the exact cause is uncertain. Note that a similar, but smaller, discrepancy can also be observed in Fig. 7(b) at $\mathrm{Re_m} \approx 9900$. The Normalised Root Mean Square Deviation (NRMSD) for the pressure drop through the cubic- and body centered structures were 2.35% and 2.43% respectively. Fig. 7 also shows that the simulation predictions for pressure drop followed the same trend as the experimental measurements. Thus, the pressure drops predicted by the CFD simulations corresponded well with the measurements made by Wentz and Thodos (1963).

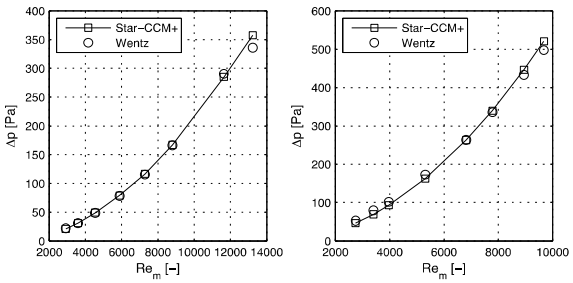

(a) Cubic structure. (b) Body centred structure.

Figure 7: Validation of CFD model results against measurements by Wentz and Thodos (1963).

Computational results

Pressure drop

Fig. 8 shows the pressure drop predictions per unit length from the CFD simulations for each bed as a function of the modified Reynolds number at different aspect ratios. It can be seen that the pressure drop over packed beds follows a distinct trend with respect to $\mathrm{Re_m}$. Also, the trend does not vary between beds with different aspect ratios, but differs only in magnitude.

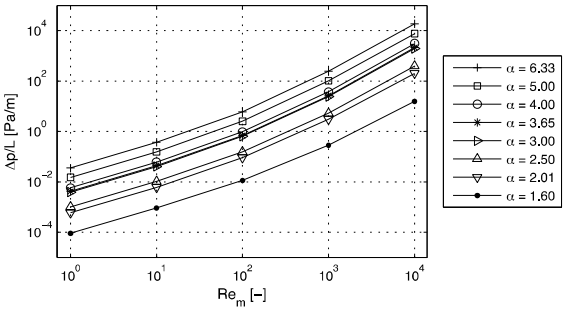

Figure 8: Pressure drop per unit length predicted by the CFD simulations as a function of $\mathrm{Re_m}$.

Friction factor

CFD simulation results are presented in terms of an integral friction factor f and compared to corresponding data from experimental measurements.
The friction factors were calculated with eqn. (5) and Fig. 9 shows the comparisons between friction factors from the CFD simulations, Ψ_{CFD}, the Eisfeld & Schnitzlein (ES) correlation, Ψ_{ES}, and the KTA correlation, Ψ_{KTA}, for the various cases that were considered.

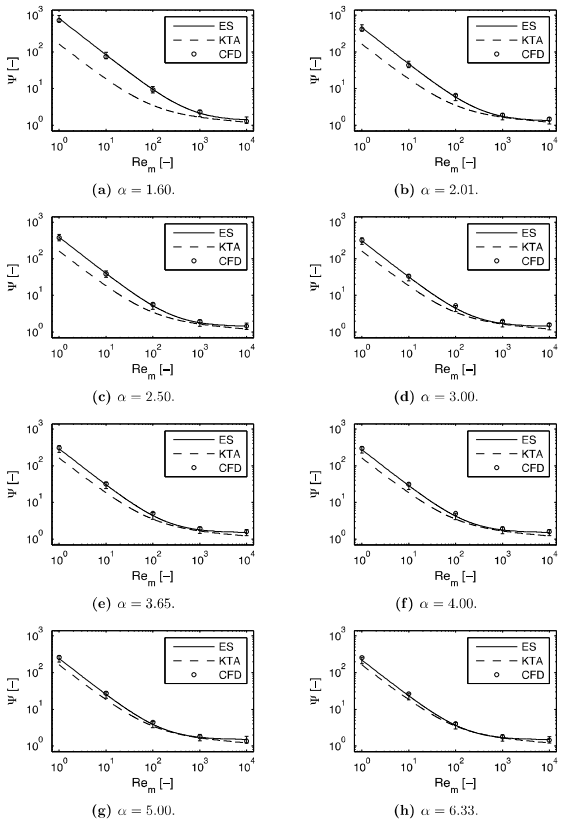

Figure 9: Comparison of friction factors between ES, KTA and CFD simulations as a function of $\mathrm{Re_m}$.

It can be seen that Ψ_{CFD} compared well with Ψ_{ES} for all instances. Ψ_{CFD} fell within the 18% NRMSD, with a confidence level of 95%, of the ES correlation. Since the ES correlation was developed from more than 2300 experimental data points, the correspondence between

Ψ_{CFD} and Ψ_{ES} is also a good indication of the validity of the CFD simulations.

However, Ψ_{KTA} did not correspond well with either Ψ_{CFD} or Ψ_{ES}, particularly at low aspect ratios and low modified Reynolds numbers. Fig. 9(a), with $\alpha = 1.60$, shows a large discrepancy between Ψ_{KTA} and Ψ_{CFD} and Ψ_{ES}. This indicates the influence of the wall effect since the ES correlation takes the wall effect into account, whereas the KTA correlation does not. As the aspect ratio increases to $\alpha = 6.33$ in Fig. 9(h), Ψ_{KTA} gradually moves closer to both Ψ_{CFD} and Ψ_{ES}, which shows the influence of the wall effect decreasing with the increase in aspect ratio. Also, Ψ_{KTA} corresponded better with Ψ_{CFD} and Ψ_{ES} at high modified Reynolds numbers than at low modified Reynolds numbers. This result gives evidence of the fact that the wall effect is Reynolds number dependent, where the pressure drop may increase in creeping flow regimes due to the additional wall friction, and decrease in turbulent regimes due to the increased porosity and permeability.

CONCLUSION

This paper described the results from CFD simulations of the flow through DEM generated packed beds. The numerical methodology was validated with results from the experimental investigation by Wentz and Thodos (1963). Good agreement was found between the CFD predictions for pressure drop, and their correlations.

The results for Ψ from the CFD simulations were compared to the predictions of Ψ from the KTA and ES correlations. It was found that at small aspect ratios, the KTA correlation under predicts the friction factor, stressing the need for a more specialized correlation such as the ES. The results also gave evidence of the fact that the wall effect is Reynolds number dependent, where the pressure drop may increase in creeping flow regimes due to the additional wall friction, and decrease in turbulent regimes due to the increased porosity and permeability. Since Ψ_{ES} compared well with Ψ_{CFD} in all instances, the conclusion was made that the ES correlation is valid within its limits.

The results presented here fulfilled the goal of the investigation, which was to determine the suitability of the Eisfeld and Schnitzlein pressure drop correlation for small aspect ratio packed beds.

ACKNOWLEDGEMENT

This work is based upon research supported by the South African Research Chairs Initiative of the Department of Science and Technology and the South African National Research Foundation.

REFERENCES

BAI, H., THEUERKAUF, J., GILLIS, P.A., and WITT, P.M. (2009), “A coupled DEM and CFD simulation of flow field and pressure drop in fixed bed reactor with randomly packed catalyst particles”, *Ind. and Eng. Chem. Research*, 48(8): 4060–4074.

BENENATI, R.F. and BROSILOW, C.B. (1962). "Void fraction distribution in beds of spheres", *AIChE Journal*, 8(3): 359–361.

CARMAN, P. (1937), “Fluid flow through granular beds”, *Transactions of the Institution of Chemical Engineers*, 15: 150–166.

CD-ADAPCO (2012), STAR-CCM+ User guide. 7ed.

CHENG, G., YU, A., and ZULLI, P. (1999), “Evaluation of effective thermal conductivity from the structure of a packed bed”, *Chemical Engineering Science*, 54(19): 4199 – 4209.

CUNDALL, P.A. and STRACK, O.D.L. (1979), “Discrete numerical model for granular assemblies”, *Geotechnique*, 29(1): 47–65.

DE KLERK, A. (2003), "Voidage variation in packed beds at small column to particle diameter ratio." *AIChE Journal*, 49(8): 2022-2029.

DI FELICE, R. and GIBILARO, L.G. (2004), “Wall effects for the pressure drop in fixed beds”, *Chemical Engineering Science*, 59(14): 3037–3040.

DOLEJS, V. and MACHAC, I. (1995), “Pressure drop during the flow of a newtonian fluid through a fixed bed of particles”, *Chemical Engineering & Processing: Process Intensification*, 34(1): 1–8.

EISFELD, B. and SCHNITZLEIN, K. (2001), “The influence of confining walls on the pressure drop in packed beds”, *Chemical Engineering Science*, 56(14): 4321–4329.

EPPINGER, T., SEIDLER, K., and KRAUME, M. (2011), “DEM-CFD simulations of fixed bed reactors with small tube to particle diameter ratios”, *Chemical Engineering Journal*, 166(1): 324–331.

ERGUN, S. (1952), “Fluid flow through packed columns”, *Chemical Engineering Progress*, 48(2): 89– 94.

HASSAN, Y.A. and KANG, C. (2012), “Pressure drop in a pebble bed reactor under high Reynolds number”, *Nuclear Technology*, 180(2): 159–173.

KTA (1988), Safety Standard by the Nuclear Safety Standards Commission, “Kerntechnischer Ausschuss”. “Bundesanzeiger”, 44: D1–D36.

MARIANI, N.J., SALVAT, W.I., CAMPESI, A., BARRETO, G.F., and MARTINEZ, O.M. (2009), "Evaluation of structural properties of cylindrical packed beds using numerical simulations and tomographic experiments", *Int. Jour. of Chem. Reactor Eng.*, 7:1.

MUELLER, G.E. (2010), “Radial porosity in packed beds of spheres”, *Powder Technology*, 203(3): 626– 633.

MUNSON, B.R., YOUNG, D.F., OKIISHI, T.H., and HUEBSCH, W.W. (2010), Fundamentals of fluid mechanics. John Wiley and Sons, Inc., 6th edition.

REDDY, R.K. and JOSHI, J.B. (2010), “CFD modeling of pressure drop and drag coefficient in fixed beds: Wall effects”, Particuology, 8(1): 37–43.

REICHELT, W. (1972), “Calculation of pressure drop in spherical and cylindrical packings for single-phase flow” (“Zur Berechnung des Druckverlustes einphasig durchstroemter Kugel- und Zylinderschuettungen”), *Chemie-Ingenieur-Technik*, 44(18): 1068–1071.

REYNEKE, H.J. (2009), “Investigation into the velocity distribution through an annular packed bed”, *M.Eng.(Nuclear)*, North-West University, South-Africa.

REYNOLDS, O. (1900), Papers on mechanical and physical subjects. Cambridge University Press, 14: 81–85.

THERON, W.G.J. (2011), “Numerical analysis of the flow distribution within packed columns using an explicit approach”, *M.Eng.(Nuclear)*, North-West University, South-Africa.

VAN DER MERWE, W.J.S. (2014), "Analysis of flow through cylindrical packed beds with small cylinder diameter to particle diameter ratios", *M.Eng.(Nuclear)*, North-West University, South-Africa.

WENTZ, C.A. and THODOS, G. (1963), “Pressure drops in the flow of gases through packed and distended beds of spherical particles”, *AIChE Journal*, 9(1): 81–84.

